The Role of Carbonate Mineral Dissolution in Turbidity Reduction in an Oil Sands End Pit Lake

Ho Yin Poon[1], *Heidi L. Cossey*[1], *Amy-lynne Balaberda*[1], and *Ania C. Ulrich*[1,*]

[1] Department of Civil & Environmental Engineering, University of Alberta, Edmonton, Alberta, Canada T6G 1H9

* Corresponding Author: Rm. 7-265 Donadeo Innovation Center for Engineering (ICE) Building, Department of Civil & Environmental Engineering, 9211-116th St NW, University of Alberta, Edmonton, Alberta, Canada, T6G 1H9. Email address: aulrich@ualberta.ca; Phone: +1 780 492 8293

Abstract

Surface water turbidity from dispersed clay particles can hinder the development of aquatic ecosystems. One of the primary objectives for proposed oil sands end pit lakes is that they support ecological functions and lake-specific wildlife habitat. However, high surface water turbidity has been observed in the Base Mine Lake cap water, the first full-scale demonstration oil sands end pit lake. Our previous study showed that adjusting the solution pH through carbon dioxide (CO_2) addition reduced surface water turbidity in oil sands tailings. Carbonate minerals such as calcite and dolomite were also previously identified in tailings, and thus the goal of this study was to determine the effect of calcite and dolomite dissolution through CO_2-mediated pH reduction on turbidity and the stability of suspended clay particles. Calcite dissolution resulted in ~99% reduction of turbidity. The suspended clay particle stability was analyzed using DLVO (Derjaguin-Landau-Verwey-Overbeek) theory with water chemistry data from this column study. An inverse correlation was observed between the amount of dolomite and the energy barrier values on day 42 of the experiment. These results suggest CO_2-mediated calcite dissolution changes the water chemistry and is the most promising treatment condition for the settlement of suspended tailings particles.

Keywords: End pit lakes, Oil sands, Turbidity, Carbon dioxide, Calcite, Dolomite

Abbreviations

BCR, Beaver Creek Reservoir; BML, Base Mine Lake; $CaCl_2$, calcium chloride; CO_2, Carbon dioxide; DDL, diffuse double layer; DLVO, Derjaguin-Landau-Verwey-Overbeek; EPL, end pit lake; FFT, fluid fine tailings; HCl, hydrochloric acid; ICDD, International Centre for Diffraction Data; ICSD, Inorganic Crystal Structure Database; ICP-OES, inductively coupled plasma-optical emission spectroscopy; NRAL, Natural Resources Analytical Laboratory; OSPW, oil sands process-affected water; SBML, synthetic Base Mine Lake; SEM, scanning electron microscope; SO_4^{2-}, sulfate; TSS, total suspended solids; XRD, x-ray diffraction

1. Introduction

Surface mining and subsequent crude oil extraction from the Canadian oil sands have produced over 1.25 billion m^3 of waste, known as tailings, which is being stored in tailings ponds (AER 2019). Tailings consist of sand, silt, and clay-sized particles and oil sands process-affected water (OSPW) that contains dissolved salts, naphthenic acids, petroleum hydrocarbons, and unrecovered bitumen (Allen 2008; Dompierre et al. 2016). Once deposited in tailings ponds, the coarse sand-sized particles in tailings tend to segregate and settle out on beaches, while the fine particles (< 44 μm) stay suspended in the ponds and develop into a stable fluid-like structure that takes decades to consolidate and dewater (Chalaturnyk et al. 2002; Kasperski and Mikula 2011). These finer tailings, referred to as fluid fine tailings (FFT), typically consist of 30-40 wt. % solids, of which 10% is greater than 44 μm, 57% is between 1–44 μm, and 33% is less than 1 μm (Dompierre et al. 2016; Voordouw 2013). To curb the growing inventory of FFT the oil sands industry is developing alternative long-term FFT management and reclamation strategies, one of

which is end pit lakes (EPLs). EPLs are constructed by overlaying OSPW on a thick layer of FFT in a decommissioned open pit. It is anticipated that EPLs will allow FFT to slowly dewater and consolidate over time while the water cap provides habitat for the development of a self-sustaining aquatic ecosystem (Westcott and Watson 2007).

In 2013, Syncrude Canada Ltd. (Syncrude) commissioned the first full-scale demonstration EPL, Base Mine Lake (BML). While periphyton, phytoplankton, zooplankton, and benthic invertebrates are present in BML (Syncrude Canada Ltd. 2017), high concentration of total suspended solids (TSS) and high turbidity (as high as 300 NTU) have also been measured in the BML water cap (Dompierre et al. 2017; Dompierre et al. 2016; Lawrence et al. 2016; Syncrude Canada Ltd. 2017), which can limit light penetration into the lake, making it difficult to establish a healthy littoral zone (Charette et al. 2010). Littoral zones are important for spawning and nesting habitat and food for organisms, protection from sun and predators, erosion control, dissolved oxygen, and water quality. Thus, turbidity may inhibit the ability of EPLs to develop into self-sustaining aquatic ecosystems. Mechanisms of turbidity reduction must be understood before full-scale implementation of EPLs.

A possible mechanism of turbidity reduction in BML is through pH-induced dissolution of carbonate minerals in FFT, which occurs as a result of biogenic carbon dioxide (CO_2) production (Poon et al. 2018; Siddique et al. 2014). Previous studies have found that lowering the pH of FFT with dissolved CO_2 can improve settlement and consolidation in fine tailings (Ibanez et al. 2014; Siddique et al. 2014). This behavior has been attributed to decreased thickness of the diffuse

double layer (DDL) surrounding suspended clay particles in FFT as a result of increased concentrations of soluble cations (Siddique et al. 2014). Decreased DDL thickness results in clay flocculation, thereby increasing clay particle settlement and consolidation. Further, studies have indicated that CO_2 addition can improve water clarity in laboratory columns containing FFT capped with 60%/40% OSPW/freshwater (Poon et al. 2018). Thus, it is hypothesized that pH-induced carbonate mineral dissolution may play an important role in BML turbidity reduction. Previous work identified calcite ($CaCO_3$) minerals in FFT and OSPW sediment samples (Poon et al. 2018). Dolomite ($CaMg(CO_3)_2$) minerals are also thought to be present in the FFT (Dompierre et al. 2016). This current study examines the role of carbonate (calcite and dolomite) mineral dissolution on turbidity reduction in the BML water cap.

2. Materials and Methods

2.1 Sample collection

Water from BML (herein referred to as BML-OSPW) and freshwater from the Beaver Creek Reservoir (BCR) were provided by Syncrude. BML-OSPW was collected from the surface layer of BML (from the southwest platform) in September 2014 and is a mixture of approximately 80% OSPW and 20% BCR fresh water. BCR was collected in October 2015. All samples were stored at 4°C until use.

2.2 Calcite and dolomite characterization

Calcite (Iceland Spar Crystal; Ward's Scientific, Inc.) and bulk dolomite (provided by Dr. Matthew Lindsay, University of Saskatchewan) samples were ground and sieved to 45–75 μm aperture mesh size to represent the size of calcite particles found within FFT (Dompierre et al.

2016; Voordouw 2013). The ground samples of calcite and dolomite were characterized before the experiment by x-ray diffraction (XRD) and scanning electron microscopy (SEM) (see Supplementary Material). XRD analysis was performed using a Geigerflex powder x-ray diffractometer equipped with a D/Tex detector. XRD data was analyzed using JADE 9.1 software, with peak locations being referenced using the International Centre for Diffraction Data (ICDD 2016) and Inorganic Crystal Structure Databases (ICSD 2017). SEM was performed using a Zeiss Sigma (300 VP-FESEM) microscope to visualize the sample surface. In addition, chemical and elemental characteristics were determined by SEM coupled with energy dispersive x-ray spectroscopy (SEM/EDS). The crushed Iceland Spar Crystal shares some physical characteristics with the calcite identified from FFT, including rhombohedral, and in crystalline form (ICSD 2017). However, cell dimensions for the crushed Iceland spar (6.3x6.3x6.3) differ slightly from the calcite identified from FFT (4.9x4.9x17).

2.3 Experimental setup

All carbonate (calcite and dolomite) dissolution experiments were conducted in 1 L glass graduated cylinder columns (Pyrex C30221L, Fisher Scientific) covered with parafilm (PM-996) to minimize evaporation. CO_2 (99.9% purity Praxair Inc.) was added to select columns using a 20 μm pore size stainless steel pump head (GA-36410649, Mandel) at a rate of 0.5 L/min. In a study by Poon et al. (2018), the authors found ~0.4 wt% total carbonate minerals in FFT and calculated that 7.5 mol of calcite was present in a 20 cm thick slice of FFT (~15 L) (assuming that calcite was the major carbonate mineral present) (Poon et al., 2018). Because calcite dissolution is a surface controlled (or surface area dependent) reaction, it was assumed that 5×10^{-3} mol/L of calcite (equivalent to 2 cm of FFT surface) contributed to dissolution in the Poon

et al. (2018) study. Based on these assumptions, calcite dissolution studies were conducted in 1 L columns using 0.5 g/L of calcite and a 60%/40% OSPW/BCR water mixture. The 60%/40% OSPW/BCR water mixture was made by diluting the BML-OSPW provided by Syncrude with BCR. This ratio was chosen based on the results of Poon et al. (2018), which found that CO_2 addition to 60%/40% OSPW/BCR water mixtures showed the most significant improvement to water clarity. This ratio is equivalent to the dilution anticipated in the BML water cap five years after BML was commissioned. A second experiment studying the effect of combined calcite and dolomite dissolution and dolomite-only dissolution was also conducted using a 60%/40% OSPW/BCR water mixture as per Table 1. For consistency, 0.5 g/L of total carbonate minerals were used for these experiments.

Finally, to investigate the impact of sulfate on calcite dissolution, a third experiment was conducted in 1 L columns using synthetic BML (SBML) water, prepared with either 400 mg/L or 50 mg/L of SO_4^{2-} to represent the range of concentrations that are commonly found in oil sands process affected water (Mahaffey and Dubé 2016). SBML water was made according to the 2016 BML water chemistry data provided by Syncrude Canada Ltd. SBML is roughly equivalent to 60%/40% OSPW/BCR. Furthermore, to evaluate the calcite dissolution sensitivity, two different amounts of calcite (0.05 g and 0.5 g) were used in the column experiment, as per Table 2. These effects will be discussed further in the Results section.

Table 1. Summary of mixed carbonate mineral (calcite and/or dolomite) dissolution experimental columns using 60%/40% OSPW/BCR

Column	Dolomite (g)	Calcite (g)	Duplicate

No Carbonate + noCO_2 *	0	0	+
No Carbonate + CO_2	0	0	+
100% Dolomite - noCO_2	0.50	0	+
100% Dolomite + CO_2	0.50	0	+
50% Dolomite - noCO_2	0.25	0.25	+
50% Dolomite + CO_2	0.25	0.25	+
25% Dolomite - noCO_2	0.13	0.38	+
25% Dolomite + CO_2	0.13	0.38	+
0% Dolomite - noCO_2	0	0.50	+
0% Dolomite + CO_2	0	0.50	+

* the No Carbonate + noCO_2 duplicate was discarded after day 7 due to column leakage

Table 2. Summary of calcite dissolution experimental columns using SBML water

Column	400 mg/L SO_4^{2-}	50 mg/L SO_4^{2-}	Calcite (g)	Duplicate
400SBML - noCO_2 + no calcite	+			
400SBML + CO_2 + no calcite	+			
400SBML - noCO_2 + 0.5g calcite	+		0.5	+
400SBML + CO_2 + 0.5g calcite	+		0.5	+
400SBML - noCO_2 + 0.05g calcite	+		0.05	+
400SBML + CO_2 + 0.05g calcite	+		0.05	+
50SBML - noCO_2 + no calcite		+		
50SBML + CO_2 + no calcite		+		
50SBML - noCO_2 + 0.5g calcite		+	0.5	+
50SBML + CO_2 + 0.5g calcite		+	0.5	+
50SBML - noCO_2 + 0.05g calcite		+	0.05	+
50SBML + CO_2 + 0.05g calcite		+	0.05	+

2.4 Geochemical analyses and modeling

The turbidity of the aqueous samples was determined using a portable turbidimeter (2100Q01, Hach). Calibration was performed before each measurement. Chemical parameters were monitored throughout the experiments, including pH, alkalinity, cations, and anions. pH was measured using an Accumet AR50 dual-channel meter (Fisher Scientific). Alkalinity was

measured using a Mettler Toledo DL53 with 0.02 N H_2SO_4 as a titrant. Cation concentrations (Ca^{2+}, Mg^{2+}, Na^{+}, and K^{+}) were determined using inductively coupled plasma-optical emission spectroscopy (ICP-OES) conducted by the Natural Resources Analytical Laboratory (NRAL) at the University of Alberta. Anion concentrations (Cl^{-} and SO_4^{2-}) were determined using ion chromatography. The water samples were subjected to zeta potential measurement using a Zetasizer Nano ZSP (Malvern Instruments Ltd.).

The water chemistry profile within the column was estimated with PHREEQCi (version 3.4.0.12927; Parkhurst and Appelo (2013)) and mineral saturation indices (SIs) were calculated using the WATEQ4F (Ball et al. 1991) thermodynamic database. The stability of suspended FFT clay particles in the columns under the various carbonate (calcite and dolomite) mineral dissolution conditions was analyzed using DLVO (Derjaguin-Landau-Verwey-Overbeek) theory.

3. Results and Discussion

3.1 Effect of calcite on turbidity

Figure 1 displays the results of the 0.5 g calcite dissolution column experiments in 60%/40% OSPW/BCR. Columns without CO_2 or calcite addition ($NoCO_2$ + No Calcite) exhibited settling that allowed for an 88.1% reduction in turbidity (final turbidity of 23.7 NTU). The extent to which calcite contributes to turbidity when dissolution does not occur ($NoCO_2$ + 0.5g Calcite) was found to be minimal, with a slightly lower 87.8% reduction in turbidity (final turbidity of 25 NTU) (Figure 1c and Table S1). The addition of CO_2 alone (CO_2 + No Calcite) considerably increased the reduction in turbidity to 95.4% (final turbidity of 9 NTU), while the addition of

CO_2 and calcite (CO_2 + 0.5 g Calcite) further increased the turbidity reduction to 98.6% (final turbidity of 3 NTU) (Figure 1c and Table S1). As surface water turbidity above 3 NTU displays an observable impact on fish predation (Birtwell 2008), the CO_2-induced dissolution of calcite could serve as a foundation for BML water turbidity management and the optimization of small-bodied fish population development.

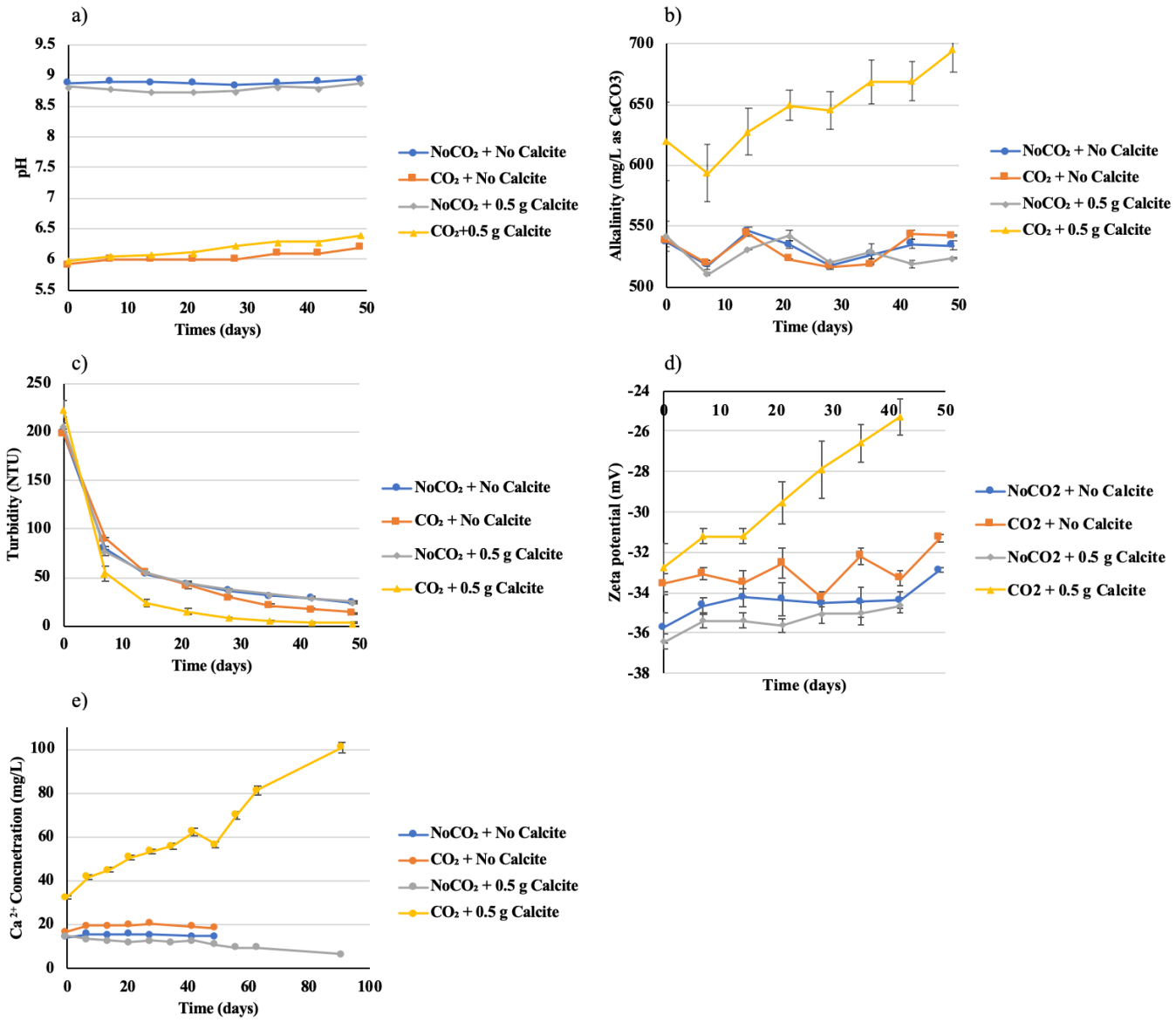

Figure 1. Physical and chemical data for the 0.5 g calcite dissolution experiments in the 60%/40% (OSPW/BCR) water mix. a) pH, b) alkalinity, c) turbidity, d) zeta potential, and e) calcium concentrations. Note: All data points are an average of duplicate columns. Error bars represent the standard error of the averaged value.

An increase in alkalinity (8%), zeta potential (22.8%), and Ca^{2+} concentration (91.6%) was observed in the CO_2 + 0.5g Calcite columns (Figures 1b, 1d and 1e and Table S1). These results further support the hypothesis that FFT dewatering can be enhanced by the release of divalent cations (Ca^{2+}) through pH-mediated calcite dissolution and subsequent reduction of the DDL thickness (Siddique et al. 2014), which was evident from the increased zeta potential. The effects of 0.5 g calcite on additional cation and anion measurements are shown in Figure S3. The Ca^{2+} concentration had only increased by ~90% by day 42 in the CO_2 + 0.5g Calcite columns (Figure 1e and Table S1). Additional water chemistry monitoring was conducted on these columns until day 91 to see if the Ca^{2+} concentration would continue to increase. After 91 days, the Ca^{2+} concentration increased by 209.5% in the CO_2 + 0.5g Calcite columns.

A linear increase in dissolved Ca^{2+} concentration with time was observed with CO_2 + 0.5g Calcite (Figure 1e), which is strongly indicative of calcite dissolution. Divalent cations such as calcium have a strong influence on DDL thickness and promote particle aggregation. In a study conducted by Ibanez et al. (2014), a linear inverse relationship between the concentration of calcium chloride ($CaCl_2$) and zeta potential was observed in a study performed with a commercially available kaolinite sample at pH 5 (adjusted by either CO_2 or hydrochloric acid (HCl)). An approximate difference in zeta potential of −7 mV was observed with two $CaCl_2$ (0.5 and 1.5 mM) concentrations tested (Ibanez et al. 2014). In our study, CO_2-mediated calcite dissolution showed a similar change in zeta potential over time; a 7 mV increase was observed for the CO_2 + 0.5 g Calcite column (day 42). The highest measured zeta potential value was −25.3 mV for the CO_2 + 0.5 g Calcite column at day 42 (Figure 1), which suggests that this

condition may be the most favorable for FFT aggregation (Ibanez et al. 2014). In a study by Zbik et al. (2008), significantly more kaolinite aggregates formed in a 0.25 mM $CaCl_2$ solution than in a 10 mM NaCl solution, both at pH 6. In addition, these authors observed that the kaolinite aggregates mainly consisted of particles connected in a butterfly shape with edge-to-edge and edge-to-face orientations with 0.25 mM $CaCl_2$ and pH 6 (Zbik et al. 2008). These observations were consistent with the general notion that approximately $1x10^{-4}$ mol/L of divalent cations are needed to induce DDL compression and destabilize particles in suspension (Hogg 2000).

To determine if the CO_2 + 0.5 g Calcite column had reached equilibrium, the predicted water chemistry and solution pH at equilibrium were calculated using PHREEQCi. Almost all of the measured pH values matched with the predicted values, however, a substantially lower dissolved calcium concentration was measured compared to the predicted values (Table 3). The measured calcium concentration was approximately 36 times less than the predicted value in the CO_2 + 0.5g Calcite column on day 42, and even with an extended experimental duration, the measured calcium concentration at day 91 was 4 times lower than the predicted value (Table 3). These results suggest that calcite equilibrium in the solution has not yet been reached. One possible reason for the apparent delay in reaching equilibrium could be due to parameters not considered during the thermodynamic calculation used by the PHREEQCi program. For example, dissolved sulfate (SO_4^{2-}) can negatively impact calcite dissolution (Compton and Brown 1994; Gledhill and Morse 2006; Sjöberg 1978).

Table 3. A comparison of calculated water chemistry with calcite dissolution and experimental results.

	Calcite				Solution parameters			
	Initial (mmole)	Final (mmole)	Saturation Index	Simulated final pH	Measured pH	Ca (mole)	Ca (mg)	Measured Ca (mg/L)
$NoCO_2$ + 0.5g Calcite	5.0	5.3	0	8.6	9.4 (Day 91)	$5x10^{-5}$	5.1	6.6 (Day 91)
CO_2 + 0.5g Calcite	5.0	4.5	0	6.3	7.3 (Day 91)	$4.6x10^{-3}$	460.4	100.8 (Day 91

3.2 Effect of mix calcite/dolomite dissolution on turbidity removal

In addition to calcite dissolution, it is expected that the dissolution of other carbonate minerals like dolomite ($MgCa(CO_3)_2$) also occurs in BML (Dompierre et al. 2016). Dompierre et al. (2016) found that BML pore water chemistry (i.e. dissolved Ca^{2+} and Mg^{2+}) and XRD results suggest the depletion of dolomite minerals. To determine whether turbidity removal can be enhanced with a mixture of calcite and dolomite, a column study using powdered dolomite samples was constructed with ratios of 100/0, 50/50, 25/75, 0/100 (% dolomite/% calcite) minerals (Table 1). Figure 2 contains the water chemistry results from the column experiments with mixtures of calcite and dolomite in 60%/40% OSPW/BCR.

Consistent pH, alkalinity, and zeta potential measurements were observed throughout the experimental period (84 days) for the $NoCO_2$ + No Calcite control columns, regardless of the addition of calcite and/or dolomite (Figure 2a, 2e, and 2g). An increase in pH was observed over time for all CO_2-treated columns and was inversely related to the amount of dolomite added,

with some exceptions when the pH of 25% dolomite columns increased slightly above that of 0% dolomite columns (Figure 2b). In columns with CO_2 treatment, alkalinity increased with the addition of dolomite and/or calcite, and columns with a high proportion of calcite (100%, 75%, and 50%) generally had higher alkalinity than columns with 100% dolomite or no carbonate minerals at all (Figure 2f).

The amount of turbidity reduction (89–91%) was similar among the $NoCO_2$ columns regardless of the presence of dolomite and/or calcite (Figure 2e and Table S2). Similar to the results discussed in Section 3.1, columns containing only calcite with CO_2 led to an improved turbidity reduction of 98% (final turbidity of 2.4 NTU) compared to the 95% reduction (final turbidity of 7.0 NTU) in columns without any carbonate minerals (Table S2). Columns containing only dolomite with CO_2 had a 97.0% reduction in turbidity (final turbidity 4.4 NTU), which is less than that of columns with calcite or mixtures of calcite and dolomite. The columns containing a dolomite/calcite mixture led to the best turbidity reduction of 98.4%, 98.2%, and 98.6% for the 0%, 25%, and 50% dolomite columns, respectively (Table S2). Columns with carbonate minerals and CO_2 exhibited higher zeta potentials compared to columns without carbonate minerals (Figure 2h). Further, columns with CO_2 treatment and 100% dolomite columns had slightly lower zeta potentials than columns containing calcite or a dolomite/calcite mixture after day 40. Dissolved ion concentrations (Ca^{2+}, Mg^{2+}) were stable for the $NoCO_2$ control columns in the 98-day period, regardless of the addition of carbonate minerals (Figures 3a and 3c). For the CO_2-treated columns, a higher increase in Ca^{2+} ion concentrations was observed with increasing amounts of calcite (Figure 3b), while only the 100% dolomite with CO_2 column displayed a

substantial increase in Mg^{2+} concentration over the 98-day period (Figure 3d). As expected, the ratio for the molar concentration of Mg^{2+} and Ca^{2+} ions was close to unity for the 100% dolomite with CO_2 column throughout the 98 day period (Figure 3e). Additional measurements of dissolved ion concentrations can be found in Figure S6.

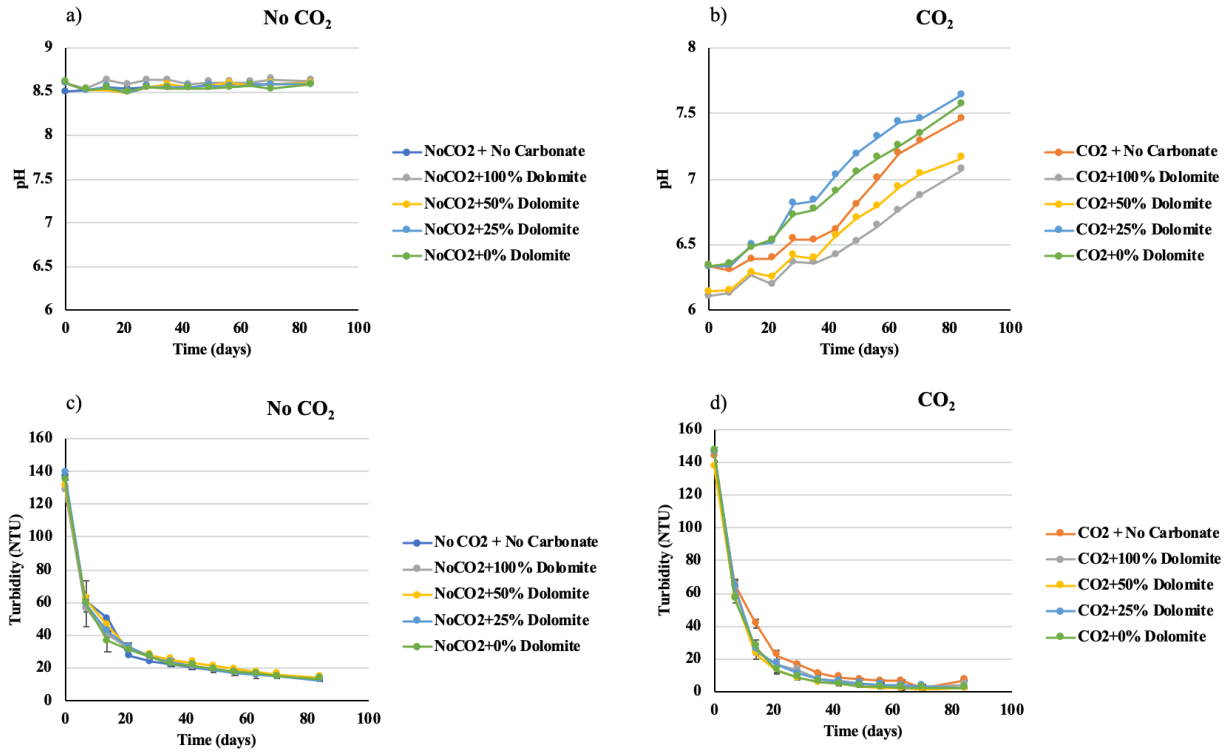

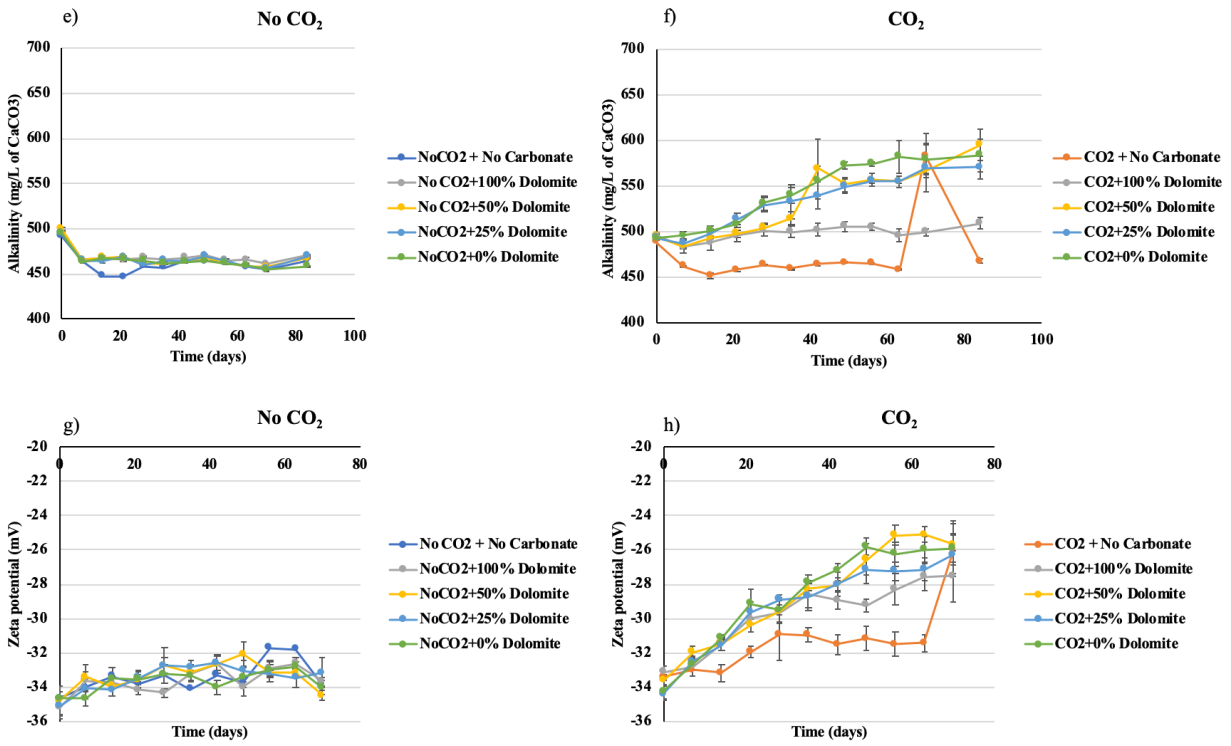

Figure 2. Physical and chemical measurements for the mixed carbonate mineral (calcite and dolomite) dissolution experiments in 60%/40% OSPW/BCR. a) pH measurements in columns with no CO_2, b) pH measurements in columns with CO_2 treatment, c) turbidity in columns with no CO_2, d) turbidity in columns with CO_2 treatment, e) alkalinity in columns with no CO_2, f) alkalinity in columns with CO_2 treatment, g) zeta potential in columns with no CO_2, and h) zeta potential in columns with CO_2 treatment. Note: All data points are an average of duplicate columns and error bars represent the standard error.

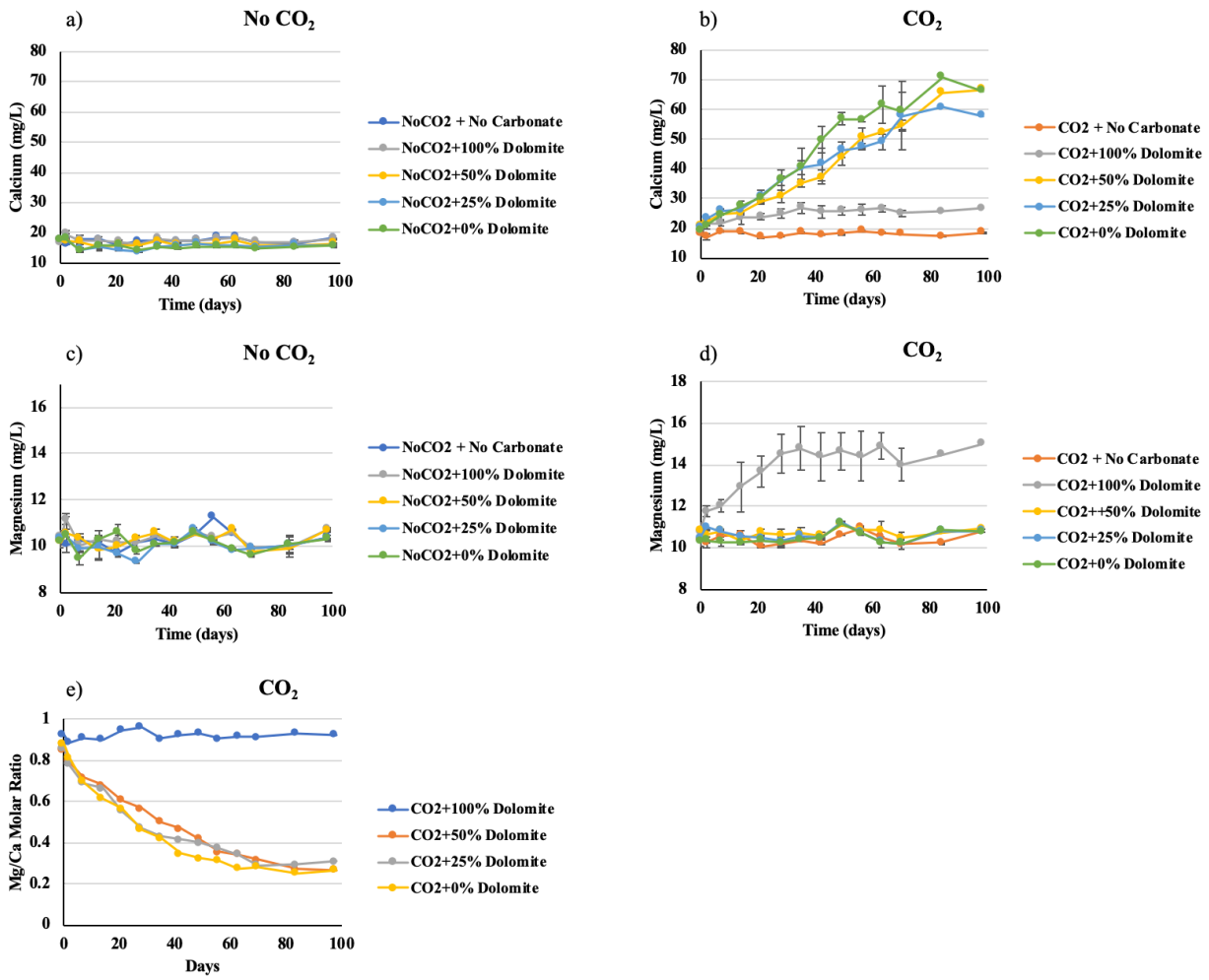

Figure 3. Dissolved ion concentrations for the mixed carbonate mineral (calcite and dolomite) dissolution experiments in 60%/40% OSPW/BCR. a) calcium concentrations for no CO_2 columns, b) calcium concentrations for CO_2 treatment columns, c) magnesium concentrations for no CO_2 columns, d) magnesium concentrations for treatment CO_2 columns, and e) Mg/Ca molar ratio for CO_2 treatment columns. Note: Averaged values were plotted except for Figure 3e, the error bars represent the standard error.

3.3 Stability of suspended clay particles

DLVO theory was applied to understand the stability of the suspended clay FFT particles under the different carbonate mineral dissolution conditions, the results of which are shown in Figure 4. DLVO theory provides a comprehensive distribution of forces between two particles, such as repulsive and attractive forces, as they relate to the particles' separation distances (Derjaguin and Landau 1993; Li et al. 2008; Missana and Adell 2000). In this study, only electrostatic repulsion and van der Waals forces were used to calculate the total interaction energy (Derjaguin and Landau 1993; Li et al. 2008; Missana and Adell 2000). A gradual decrease in the total interaction energy was observed in all columns from day 0 to day 42 (Figure 4 and S7), which correlates with the observed turbidity reduction. Interestingly, an increase in the total interaction energy was observed on day 70 for the columns with added carbonate minerals (Figures 4 and S7). The highest total interaction energy was observed at a particle separation distance of approximately 20 nm in all the columns tested, suggesting that additional energy is needed to bring the clay particles close together. The $NoCO_2$ columns had similar total interaction energy levels (~20-25 kT) that needed to be overcome for particle aggregation, regardless of the addition of carbonate minerals, while CO_2 columns without carbonate minerals had total interaction energy levels of 20 kT. The addition of carbonate minerals to CO_2-treated columns considerably decreased the energy required for particles to aggregate (~11-15 kT) on day 42 (Figure 4e). Increasing the amount of calcite decreased the total interaction energy levels, lowering the energy barrier required for the particles to flocculate. Therefore, with the addition of calcite, particle aggregates are more likely to form and improve FFT settling. However, since only the electrostatic repulsion and van der Waals forces were considered in this experiment, these results might not be applicable under more dynamic conditions such as in BML. Future work should elucidate the

contribution of other forces to total interaction energy and particle aggregation under more complex conditions. Figure S7 displays the total interaction energy results for additional columns, particularly $NoCO_2$ columns.

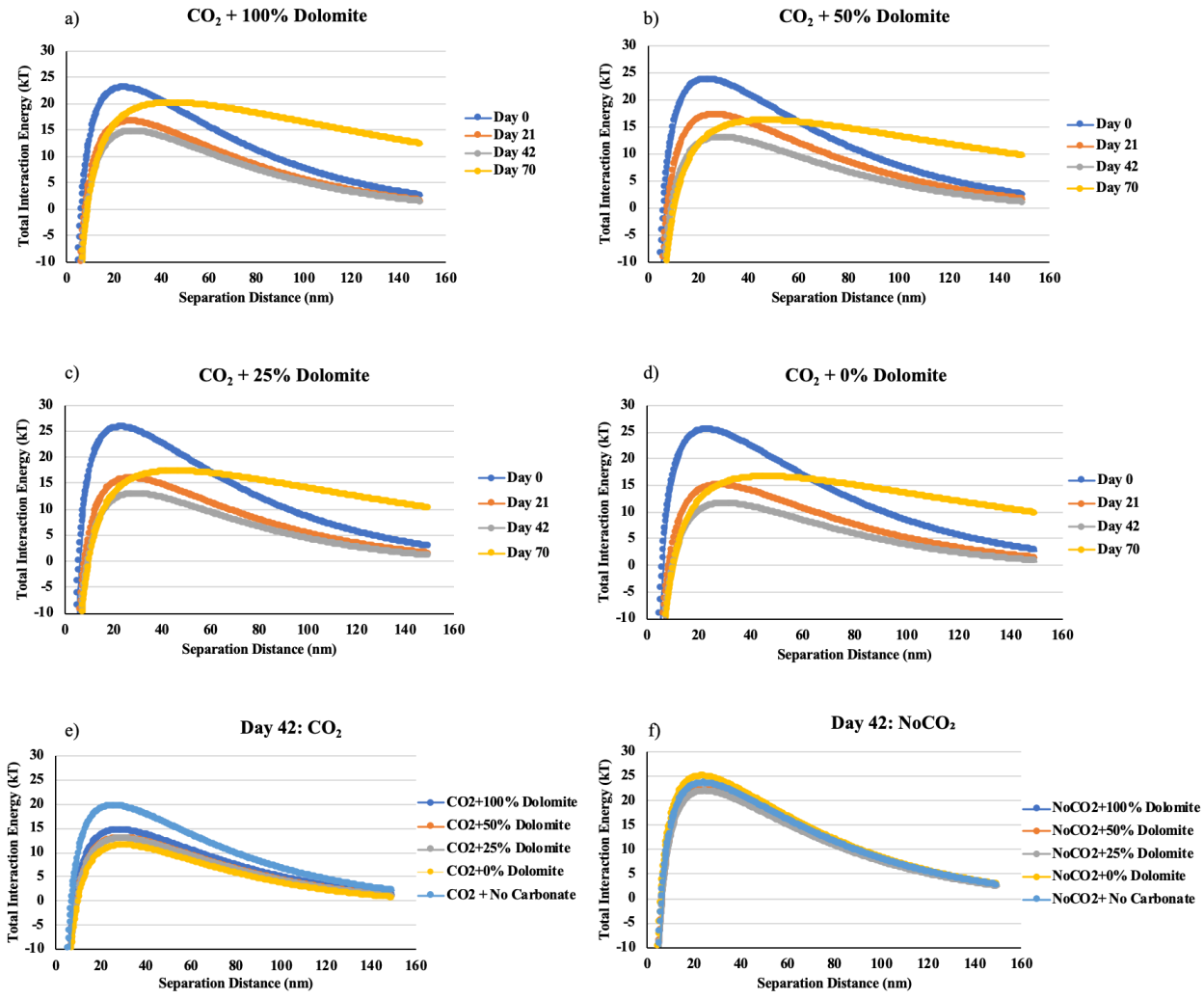

Figure 4. Total interaction energy as a function of interparticle distance for CO_2 treated columns with 60%/40% OSPW/BCR and a) 100% dolomite, b) 50% dolomite, c) 25% dolomite, d) 0% dolomite; and interaction energy profile for day 42 for columns with e) CO_2 treatment and f) no CO_2.

3.4 Effect of sulfate concentration on calcite dissolution

Figure 5 displays the results of the calcite dissolution column experiments in SBML. As mentioned in the Materials and Methods section, the effects of sulfate on calcite dissolution were investigated by adding either 400 mg/L or 50 mg/L of SO_4^{2-} to the SBML water (as per Table 2). Similar to the 60%/40% OSPW/BCR column results, CO_2 treatment initially lowered the solution pH, which then increased gradually during the 126 days, with the columns containing 400 mg/L of SO_4^{2-} exhibiting a faster increase in pH, particularly in the 400SBML + CO_2 + 0.05g calcite column (Figures 5a and b). Elevated alkalinity was observed in the CO_2 + calcite columns (0.5 g and 0.05 g calcite; Figures 5c and d). Despite a similar initial alkalinity in these columns, the alkalinity increased slightly from days 0 to 42 in the columns containing 400 mg/L SO_4^{2-} compared to those with 50 mg/L SO_4^{2-} (Figures 5c and d). While no significant change occurred in sulfate concentrations (Figure S8), dissolved Ca^{2+} displayed an interesting trend (Figures 5e and f). A spike in the Ca^{2+} concentration was observed between days 50 and 63 for 50SBML + CO_2 + 0.5g calcite column and between days 45 and 84 for 400SBML + CO_2 + 0.5g calcite column (Figure 5e). Conversely, an approximate 5.6-fold reduction in Ca^{2+} ion concentration was observed in the NoCO_2 columns, largely as a result of calcite precipitation (Figure 5f).

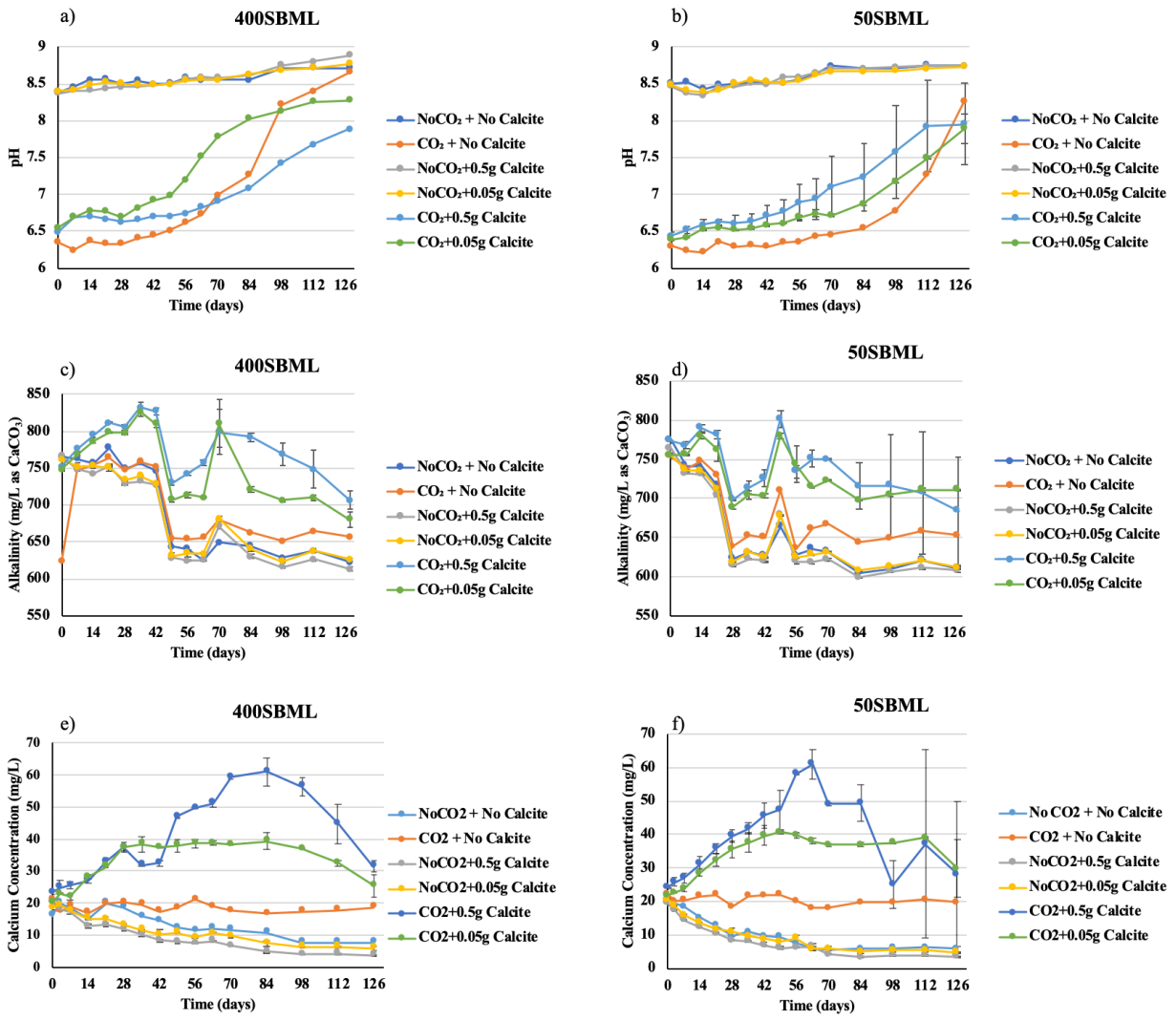

Figure 5. Water chemistry results for calcite dissolution experiment in SBML water. a) pH measurements in columns with 400 mg/L SO_4^{2-}, b) pH measurements in columns with 50 mg/L SO_4^{2-}, c) alkalinity in columns with 400 mg/L SO_4^{2-}, d) alkalinity in columns with 50 mg/L SO_4^{2-}, e) calcium concentrations in columns with 400 mg/L SO_4^{2}, and f) calcium concentrations in columns with 50 mg/L SO_4^{2-}. Note: All data points are an average of duplicate columns. Error bars represent the standard error of the averaged value.

The maximum dissolution rate for the 400 SBML + CO_2 + 0.5g calcite column was observed to be 2.9×10^{-5} mol/L/d and occurred between days 63 and 70 (Figure S9). For the 50SBML + CO_2 + 0.5g calcite column, the maximum calcite dissolution rate of 3.8×10^{-5} mol/L/d was observed between days 49 and 56. A 23.6% higher maximum dissolution rate was observed for the 50SBML + CO_2 + 0.5g calcite column (days 49-56) than for the 400SBML + CO_2 + 0.5g calcite column (days 63-70). Comparing the average dissolution rates over the 126 day period, 2.08×10^{-6} mol/L/d for the 400SBML + CO_2 + 0.5g column and 1.14×10^{-5} mol/L/d for the 50SBML + CO_2 + 0.5g calcite column, the column with 50 mg/L of SO_4^{2-} had a higher dissolution rate by 8.2%. These results are consistent with previous observations made by Gledhill and Morse (2006), who reported a 20% reduction in the calcite dissolution rate in a solution that contained 1 g/L SO_4^{2-}. Taken together, these results and those in the current study suggest that calcite dissolution occurs sooner at lower SO_4^{2-} concentrations (50 mg/L) in the presence of 0.5 g calcite. However, in the presence of 0.05 g calcite, there are no notable differences in the dissolution rates between columns with CO_2 and either 50 or 400 mg/L SO_4^{2-}.

4. Conclusions

This study indicates that the dissolution of carbonate minerals (calcite and/or dolomite) through CO_2-mediated pH reduction can reduce turbidity caused by fine particles. In columns with a 60%/40% OSPW/BCR water mixture, CO_2 + 0.5 g calcite treatment resulted in a turbidity reduction of 98.6% (final turbidity of 3 NTU), compared to 95.4% for CO_2 + No Calcite columns and roughly 88% for NoCO_2 columns. While CO_2 + 0.5 g dolomite resulted in turbidity reductions of only 97%, 0.5 g mixtures of calcite and dolomite (25% dolomite/75% calcite and

50% dolomite/50% calcite) in CO_2 treatment columns resulted in greater turbidity reductions of 98.2% and 98.6% respectively. However, a lower total interparticle interaction energy, calculated using DLVO theory, was estimated for the CO_2-treated column containing only calcite. Therefore, calcite addition is more likely to promote particle aggregation than mixtures of calcite and dolomite or dolomite alone. The inhibitory effects of sulfate on calcite dissolution were investigated and it was found that SBML containing 400 mg/L SO_4^{2-} had a lower calcite dissolution rate than SBML 50 mg/L SO_4^{2-} when comparing both average and maximum dissolution rates. Therefore, the inhibitory effect of sulfate is an important consideration for any future studies on coagulation, flocculation, and settling in oil sands pit lakes containing OSPW or FFT. Additional studies should 1) confirm the optimal SO_4^{2-} concentration to maximize calcite dissolution, and 2) apply more complex interactions to calculate the interaction energy (DLVO) so that it reflects the possible forces which particles encounter in the BML.

Data Availability Statement

All data generated or used during the study appear in the submitted manuscript or the Supplemental Data.

Acknowledgements

This work was supported by NSERC Collaborative Research and Development Grants (476652) and Syncrude Canada Ltd. We would also like to thank Dr. Matthew Lindsay from the University of Saskatchewan, and Dr. Alsu Kuznetsova, Katie Nichols, Konstantin Von Gunten, and Dr. Petr Kuznetsov from the University of Alberta for their technical assistance.

CRediT authorship contribution statement

Ho Yin Poon: Conceptualization, Methodology, Investigation. Heidi L Cossey: Writing – original draft, review, and editing. Amy-lynne Balaberda: Writing – original draft, review, and editing. Ania C Ulrich: Supervision, Funding acquisition.

Declaration of Interest: none

References

Alberta Energy Regulator (AER), 2019. State of fluid tailings management for mineable oil sands, 2018. Alberta Energy Regulator, Calgary, Alberta, Canada.

Allen, E.W., 2008. Process water treatment in Canada's oil sands industry: II. A review of emerging technologies. J. Environ. Eng. Sci. 7, 123-138.

Ball, J. W., Nordstrom, D.K., 1991. User's manual for WATEQ4F, with revised thermodynamic database and test cases for calculating speciation of major, trace, and redox elements in natural waters. United States Geological Survey, Menlow Park, California, United States.

Birtwell, I. K., Farrell, M. A., Jonsson, A., 2008. The validity of including turbidity criteria for aquatic resource protection in land development guidelines (Pacific and Yukon Region), Fisheries and Oceans Canada, Ottawa, Ontario, Canada.

Chalaturnyk, R.J., Scott, J.D., Özüm, B., 2002. Management of oil sands tailings. Pet. Sci. Technol. 20, 1025-1046.

Charette, T., Castendyk, D., Hrynyshyn, J., Küpper, A., McKenna, G., Mooder, B., 2010. End pit lakes guidance document 2012. Cumulative Effects Management Association, Fort McMurray, Alberta, Canada.

Compton, R. G., Brown, C. A., 1994. The inhibition of calcite dissolution precipitation – Mg^{2+} cations. J. Colloid Interf. Sci. 165(2), 445-449. doi:DOI 10.1006/jcis.1994.1248

Derjaguin, B., Landau, L., 1993. Theory of the stability of strongly charged lyophobic sols and of the adhesion of strongly charged-particles in solutions of electrolytes. Prog. Surf. Sci. 43(1-4), 30-59. doi:Doi 10.1016/0079-6816(93)90013-L

Dompierre, K. A., Barbour, S. L., North, R. L., Carey, S. K., Lindsay M. B. J., 2017. Chemical mass transport between fluid fine tailings and the overlying water cover of an oil sands end pit lake. Water Resour. Res. 53(6), 4725-4740. doi:10.1002/2016wr020112

Dompierre, K. A., Lindsay, M. B. J., Cruz-Hernandez, P., Halferdahl, G. M., 2016. Initial geochemical characteristics of fluid fine tailings in an oil sands end pit lake. Sci. Total Environ. 556, 196-206. doi:10.1016/j.scitotenv.2016.03.002

Gledhill, D. K., Morse, J. W., 2006. Calcite dissolution kinetics in Na-Ca-Mg-Cl brines. Geochim. Cosmochim. Acta. 70(23), 5802-5813. doi:10.1016/j.gca.2006.03.024

Hogg, R. (2000). Flocculation and dewatering. Int. J. Miner. Process. 58(1-4), 223-236. doi:Doi 10.1016/S0301-7516(99)00023-X

Ibanez, M., Wijdeveld, A., Chassagne, C., 2014. The role of mono- and divalent ions in the stability of kaolinite suspensions and fine tailings. Clay Clay Miner. 62(5-6), 374-385. doi:10.1346/Ccmn.2014.0620502

Inorganic Crystal Structure Database (ICSD), 2017. ICSD web (database). FIZ Karlsruhe – Leibniz Institute for Information Infrastructure, Eggenstein-Leopoldshafen, Germany.

International Centre for Diffraction Data (ICDD), 2016. PDF-4+ 2016 (database), edited by K. Soorya. Newtown Square, Pennsylvania.

Kasperski, K.L., Mikula, R.J., 2011. Waste streams of mined oil sands: characteristics and remediation. Elements. 7, 387-392.

Lawrence, G. A., Tedford, E. W., Pieters, R., 2016. Suspended solids in an end pit lake: potential mixing mechanisms. Can. J. Civ. Eng. 43(3), 211-217. doi:10.1139/cjce-2015-0381

Li, Q., Jonas, U., Zhao, X. S., Kapp, M., 2008. The forces at work in collodial self-assembly: a review on fundamental interactions between collodial particels. Asia-Pac. J. Chem. Eng. 3(3), 255-268. doi:10.1002/apj.144

Mahaffey, A., Dubé, M., 2017. Review of the composition and toxicity of oil sands process-affected water. Environ. Rev. 25(1), 97-114.

Missana, T., Adell, A., 2000. On the applicability of DLVO theory to the prediction of clay colloids stability. J. Colloid Interf. Sci. 230(1), 150-156. doi:10.1006/jcis.2000.7003

Parkhurst, D. L., Appelo, C.A.J., 2013. Description of input and examples for PHREEQC version 3: A computer program for speciation, batch-reaction, one-dimensional transport, and inverse geochemical calculations. US Department of the Interior, United States Geological Survey, Denver, Colorado, United States.

Poon, H. Y., Brandon, J. T., Yu, X. X., Ulrich, A. C., 2018. Turbidity mitigation in an oil sands pit lake through pH reduction and fresh water addition. J. Environ. Eng. 144(12). doi:Artn 04018127 10.1061/(Asce)Ee.1943-7870.0001472

Siddique, T., Kuznetsov, P., Kuznetsova, A., Arkell, N., Young, R., Li, C., Guigard S., Underwood E., Foght, J. M., 2014. Microbially-accelerated consolidation of oil sands tailings. Pathway I: changes in porewater chemistry. Front. Microbiol. 5, 106. doi:10.3389/fmicb.2014.00106

Sjöberg, E. L., 1978. Kinetics and mechanism of calcite dissolution in aqueous solutions at low temperatures. Almqvist & Wiksell, Stockholm, Sweden.

Syncrude Canada Ltd., 2017. 2016 Summary Report: Base Mine Lake Monitoring and Research Program. Submitted to Alberta Energy Regulator, Calgary, Alberta, Canada.

Voordouw, G., 2013. Interaction of oil sands tailings particles with polymers and microbial cells: First steps toward reclamation to soil. Biopolymers. 99(4), 257-262. doi:10.1002/bip.22156

Westcott, F., Watson, L., 2007. End pit lakes technical guidance document. Clearwater Environmental Consultants for Cumulative Effects Management Association End Pit Lakes Subgroup, Project 2005-61, Calgary, Alberta, Canada.

Zbik, M. S., Smart, R. S. C., Morris, G. E., 2008. Kaolinite flocculation structure. J. Colloid Interf. Sci. 328(1), 73-80. doi:10.1016/j.jcis.2008.08.063